HOSTED BY

ELSEVIER

Available online at www.sciencedirect.com

ScienceDirect

journal homepage: http://ees.elsevier.com/ejbas/default.asp

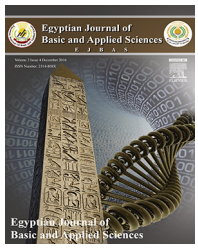

Full Length Article

Selective synthesis of acetone from isopropyl alcohol over active and stable CuO–NiO nanocomposites at relatively low-temperature

Abd El-Aziz A. Said *, *Mohamed M.M. Abd El-Wahab*, *Mohamed N. Goda*

Chemistry Department, Faculty of Science, Assiut University, 71516 Assiut, Egypt

ARTICLE INFO

Article history:
Received 5 May 2016
Received in revised form 17 August 2016
Accepted 26 August 2016
Available online 5 September 2016

Keywords:
CuO–NiO
Nanocomposites
Electrical conductivity
Isopropanol
Acetone

ABSTRACT

CuO–NiO nanocomposite catalysts were synthesized by an oxalate precipitation route. The basicity of the catalysts was measured using adsorption–desorption of acetic acid. The catalytic conversion of isopropanol to acetone was carried out in a conventional fixed bed flow type reactor at 200 °C using N_2 as a carrier gas. The results indicated that, the addition of NiO to CuO greatly enhanced the electrical conductivity via the creation of new charge carriers (Cu^{+}–Ni^{3+}). In addition, the results revealed that the catalyst containing 30 wt.% NiO calcined at 400 °C possesses the highest catalytic activity with 98% conversion and 100% selectivity to acetone. The remarkable catalytic performance of the synthesized catalysts is attributed to the decrease of the energy gap, the increase in the concentration of charge carries (Cu^{+}–Ni^{3+}), and to the creation of more weak and intermediate basic sites.

1. Introduction

Acetone is an important material in many laboratory and industrial applications such as, a chemical intermediate in pharmaceuticals and as a solvent for vinyl and acrylic resins, lacquers, alkyd paints, inks, cosmetics and varnishes. It is also used in the preparation of paper coatings, adhesives, and heat-seals coatings and is also employed as starting material in the synthesis of many compounds [1–3]. Acetone can be produced industrially via two routes, the first is the cumene hydroperoxide oxidation and the second is the dehydrogenation of isopropyl alcohol (IPA). It is estimated that, at present, nearly 85% of acetone world capacity is based on cumene hydroperoxide route for the co-production of acetone and phenol. About 0.62 tons of acetone is produced per ton of phenol obtained. The production of acetone from only cumene would require a balancing of the market with the phenol product from this process. Therefore, there is a need of alternative routes for acetone production other than the cumene process.

* *Corresponding author.*
E-mail address: aasaid55@yahoo.com (A.E.-A.A. Said)
http://dx.doi.org/10.1016/j.ejbas.2016.08.004

Dehydrogenation of IPA over a metal, metal oxide or salt catalysts is the second route for the manufacture of acetone. The preparation of nanostructured materials has received considerable attention owing to their unique properties and interesting potential applications [4–10]. Metal oxide nanomaterials are interesting solids due to their surface acid–base properties and oxidation–reduction potentials and hence they constitute the largest family of heterogeneous catalysts [11–16]. Several transition metal oxides exhibit the oxidation–reduction behavior due to the ease with which they can be used as an oxidizing agent and then readily be generated [17–21]. In this context, Turton et al. [22] mentioned that a single pass conversion of 85–92% with respect to IPA with reactor conditions of 2 bars and 350 °C is generally achieved. El-Shobaky et al. [23] have studied the catalytic conversion of IPA over CuO/MgO treated with K_2O. They stated that the investigated system behaved as selective catalyst for dehydrogenation of isopropyl alcohol. In addition, the surface properties, catalytic activities, and catalytic selectivities toward IPA conversion of NiO/Al_2O_3 and CuO/Al_2O_3 catalysts were investigated by Ashour [24]. The author concluded that the conversion of isopropanol at a reaction temperature of 260–350 °C proceeded to propene and to acetone with different selectivities. Moreover, the influence of precursor of MgO and preparation conditions on the catalytic dehydrogenation of IPA over CuO/MgO catalysts has been studied by El-Molla et al. [25]. Furthermore, the physicochemical properties of individual and binary Ni and Ce oxide systems have been studied by Deraz and Al-Arifi [26]. They concluded that at a reaction temperature of 250–450 °C, NiO and also CeO_2 acted as dehydrogenation catalysts whereas their mixture containing 12 wt.% NiO acted as dehydrogenation and a dehydration catalyst for isopropanol conversion. The maximum conversion obtained was 47% at a reaction temperature of 450 °C with selectivity to acetone of 62.2%. The surface and catalytic properties of NiO/MgO system doped with Fe_2O_3 have been studied by Shaheen et al. [27] and they concluded that pure and variously doped solids behave as dehydrogenation and dehydration catalysts leading to the formation of acetone and propene.

In our previous work [28], CuO–NiO mixed nanocomposites were synthesized by oxalate route and the catalysts were characterized by TG, DTA, XRD, TEM, nitrogen sorption and surface excess oxygen.

However, the highly catalytic conversion of IPA selectively to acetone over nano CuO–NiO mixed oxide systems, to our knowledge, has not yet been reported. Therefore, the challenge of this work was devoted to synthesize acetone from IPA over CuO–NiO nanocomposites as competitive catalysts with those previously reported.

2. Experimental

2.1. Materials

Acetone, ethanol and oxalic acid dihydrate were of analytically pure reagent and were used without further purification. Copper nitrate $Cu(NO_3)_2.3H_2O$ and nickel nitrate $Ni(NO_3)_2.6H_2O$ were supplied by WINLAB company for laboratory chemicals (>99%).

2.2. Preparation of pure and mixed oxide nanocomposites

Pure Nano CuO and NiO were prepared by precipitation method as described previously [12,28–30]. The precipitates were dried in the air overnight at room temperature to get the precursors. Pure CuO and NiO were obtained by calcination of their precursors from 400 up to 700 °C in a muffle furnace under air atmosphere for 3 h. CuO–NiO mixed oxide systems were prepared by co-precipitation method as described previously. The CuO–NiO nanocomposites with different ratios of NiO (1–50 wt.%) were obtained by annealing their precursors from 400 up to 700 °C in a muffle furnace under air atmosphere for 3 h.

2.3. Apparatus and techniques

2.3.1. Electrical conductivity

The electrical conductivity measurements were carried out with the method described by Said et al. [31]. The powder sample is compressed between two platinum discs whose ends are connected to the electrometer. The whole sample is then placed inside an electric oven which opens along its generatrix. The oven is of a non-inductive type and has no temperature gradient in its central part. A temperature controller is adjusted within ±1 °C in the range of 100–300 °C. A Keithley Electrometer model 610 C instrument is used for measuring the resistivity.

2.3.2. Determination of basic sites

The basicity of pure CuO, pure NiO and CuO mixed with 30 wt.% NiO catalysts calcined at 400 °C was investigated by the saturation of the basic sites with acetic acid according the following procedure: After measuring the conversion activity of IPA at steady state conditions over the investigated catalysts, at a reaction temperature of 200 °C, the catalyst was injected with different volumes of glacial acetic acid in the stream of reactants using N_2 as a carrier gas and following up the activity variations. Moreover, the strength of the basic sites was studied by following up the change in the catalytic activity of IPA with the desorption of acetic acid from the presaturated samples with time at 200 °C.

2.3.3. Catalytic activity

The activity of the catalysts toward dehydrogenation of isopropyl alcohol (IPA) in the gas phase was carried in a conventional fixed bed flow type reactor. The gases after reaction were chromatographically analyzed by an FID on a Unicam ProGc using 10% PEG 400 glass column (2 m). The reaction conditions were: 0.5 g catalyst weight, 1.6% IPA reactant was fed into the reactor after nitrogen had been bubbled through thermostated IPA at a total flow rate of 110 mL min^{-1} and the reaction temperature was 200 °C. The measurements of conversion, yield and selectivity (in %) were made after 1.5 h to achieve steady state conditions.

3. Results and discussion

3.1. Electrical conductivity measurements

The electrical conductivity measurements of the pure CuO, pure NiO and CuO–NiO mixed nanocomposite catalysts calcined at

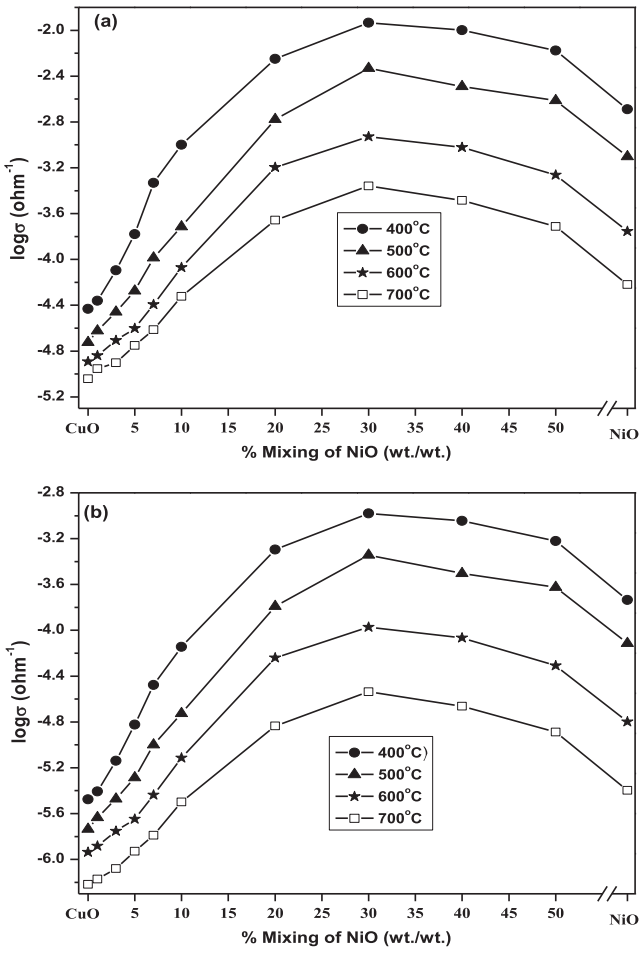

Fig. 1 – Variation of log σ with the % mixing of NiO for CuO–NiO nanocomposites calcined at 400–700 °C (a) without isopropyl alcohol, and (b) with isopropyl alcohol.

400–700 °C are carried out and graphically presented in Fig. 1(a). The results show that the electrical conductivity of the pure NiO is higher than that of CuO whereas both conductivities are lower than that of the mixed oxide nanocomposites for all calcination temperatures. In addition, the electrical conductivity of the CuO–NiO mixed oxide systems increases with increasing the wt.% NiO reaching the maxima at 30%. Above this maxima, there is a continuous decrease in the conductance values with further increase of NiO up to 50 wt.%. Moreover, upon increasing the calcination temperature from 400 up to 700 °C, log σ values decrease for the pure and mixed catalysts.

However, it is well known that CuO is a p-type semiconductor [32] and its electrical conductivity is due to the presence of Cu^{+} ions in its non-stoichiometric structure. Also, NiO behaves also as a p-type semiconductor and its p-typeness exists from a hopping mechanism [33] via an electron transfer between Ni^{3+} and Ni^{2+}. So, the observed increase in the electrical conductivity of the CuO–NiO mixed oxide systems may be attributed to the increase in the concentration of charge carriers (Ni^{3+} and Cu^{+}) [34,35]. The creation of these charge carriers due to a synergistic effect [17,36–38] can be explained according to the following proposed mechanistic synergism:

$$2CuO + 2NiO \rightarrow Cu_2O + Ni_2O_3 \quad (1)$$

or

$$Cu^{2+} + Ni^{2+} \rightarrow Cu^{+} + Ni^{3+} \quad (2)$$

On the other hand, the decrease in the electrical conductivity of the CuO–NiO mixed oxides upon increasing the wt.% NiO above 30 may correspond to a possible decrease in the mobility of charge carriers [37]. The observed decrease in the electrical conductivity values of the pure and mixed oxide nanocomposites upon increasing the calcination temperature from 400 to 700 °C may be attributed to the decrease in the values of S_{BET} [28,39,40].

The effect of IPA vapor admission on the electrical conductivity of the pure oxides and CuO–NiO mixed catalysts calcined at different temperatures has been studied and the results are shown in Fig. 1(b). The experimental conditions used are similar to that used in catalytic activity runs. The results indicated that a similar trend (as in Fig. 1(a)) was observed, but with lower log σ values. This behavior entirely reflects that IPA reactant decreases the charge carriers (Cu^{+} and Ni^{3+}) created in these catalysts via the electrons injected from IPA [40].

On the other hand, it was established that the value of activation energy provides a better information about the conductivity changes. Therefore, log σ values were plotted as a function of the reciprocal of absolute temperature and the activation energies ΔE_σ were calculated from the slope of the straight lines of the following Arrhenius relationship [41].

$$\sigma = \sigma^{*} e^{-\Delta E\sigma/KT} \quad (3)$$

where σ is the electrical conductivity, σ^{*} is the pre-exponential factor, ΔE_σ is the activation energy by conduction, K is the Boltzmann constant and T is the absolute temperature.

The graphical representations of the linear form of the Arrhenius plot for each sample are given in Fig. 2(a–c). It can be seen from these figures that log σ varies linearly against 1/T for the pure and mixed oxide systems, indicating that one and the same conduction mechanism is established for all the investigated samples in the temperature range of 100–300 °C. Values of ΔE_σ are obtained by least square fitting of the obtained lines.

The activation energy values of the electrical conduction of the catalysts under investigation (with and without IPA) are calculated and cited in Table 1. The results reveal that the values of ΔE_σ of pure oxides in the absence of IPA possess the highest values. Upon mixing CuO with 30 wt.% NiO, the activation

Table 1 – Activation energy values (with and without IPA) for pure CuO, pure NiO and CuO mixed with 30 wt.% NiO nanocomposites calcined at 400 °C.

Catalyst	ΔE_σ (eV)	
	Without IPA	With IPA
Pure CuO	0.83	0.79
CuO mixed with 30 wt.% NiO	0.12	0.03
Pure NiO	0.50	0.40

IPA: Isopropyl alcohol.

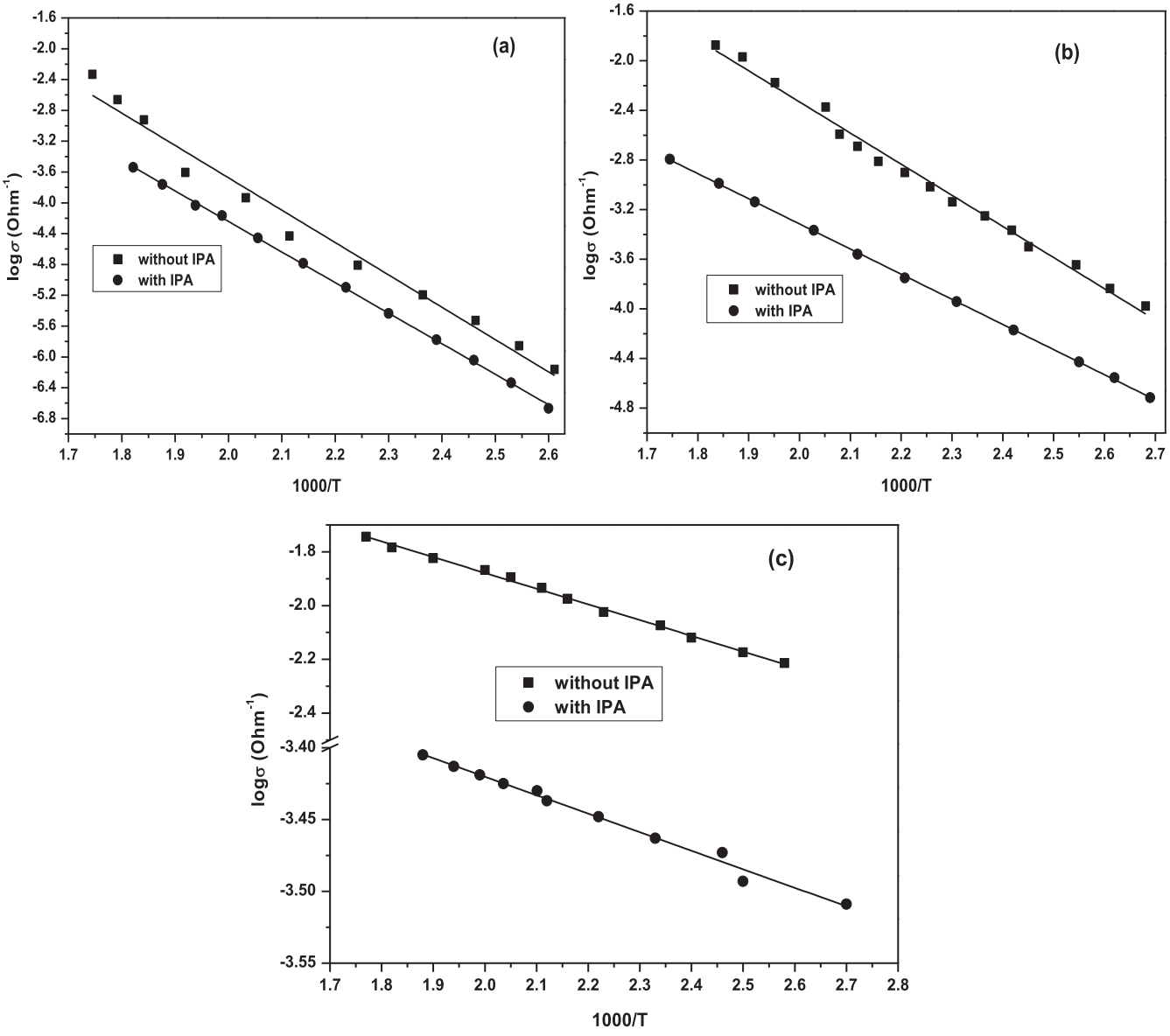

Fig. 2 – Variation of log σ versus 1/T for (a) pure CuO, (b) pure NiO, and (c) CuO mixed with 30 wt.% NiO, nanocomposites calcined at 400 °C.

energy progressively decreases, reaching to (0.12 eV). This decrease in ΔE_σ value of CuO mixed with 30 wt.% NiO catalyst reflects again the pronounced increase in the creation of the charge carriers (Cu^+ and Ni^{3+}). On the other hand, the activation energy values measured in the presence of IPA indicated that the ΔE_σ variation with NiO loading exhibits similar behavior, but with lower values than that measured in the absence of IPA. The reason for such behavior is due to the injected electrons by IPA into the catalyst surface during the dehydrogenation process [35]. These electrons are trapped in or on the catalyst surface, causing a downward bending of the conduction band toward the Fermi level and consequently decrease the activation energy ΔE_σ. Therefore, the decrease of ΔE_σ should facilitate the electron exchange between the conduction and valence bands [42]. Moreover, its width is an important factor in controlling the redox mechanism, the number of chemisorbed molecules in the course of a catalytic reaction and the nature of the chemical bonds formed between the molecules and the catalyst surface. These factors control at the same time the activity and selectivity of the catalyst as well as the mechanism of the catalytic reaction.

3.2. *Basicity of catalysts*

Saturation of the active basic sites by acetic acid over pure oxides and CuO mixed with 30 wt.% NiO catalysts calcined at 400 °C during the IPA conversion was studied and the results obtained are represented in Fig. 3(a–c). Curve (a) shows the influence of acetic acid additions on the catalytic dehydrogenation of IPA over NiO catalyst. It appears that the saturation of the basic sites on NiO by acetic acid was obtained after injection of 1.8 μL. In addition, the IPA conversion decreases from 44% to 1% with increasing the volume of acetic acid up to 3 μL. Curve (b) shows the influence of acetic acid injection on the IPA

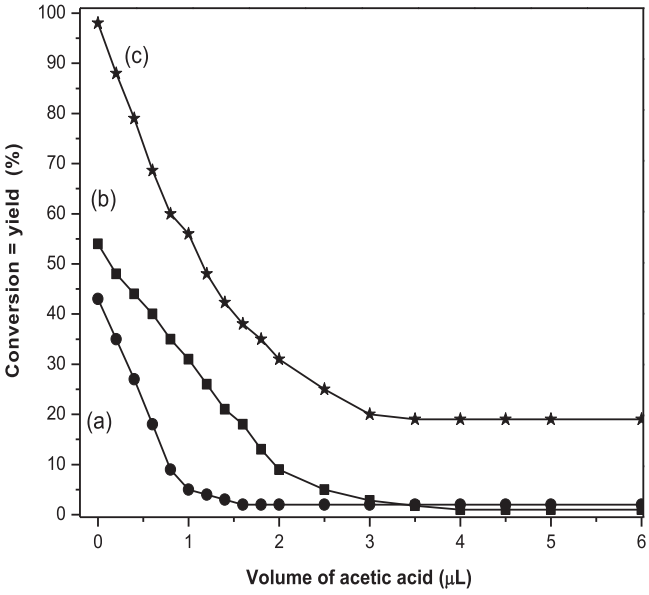

Fig. 3 – Effect of acetic acid injections on the catalytic conversion of IPA to acetone over (a) pure NiO, (b) pure CuO and (c) CuO mixed with 30 wt.% NiO nanocomposites calcined at 400 °C.

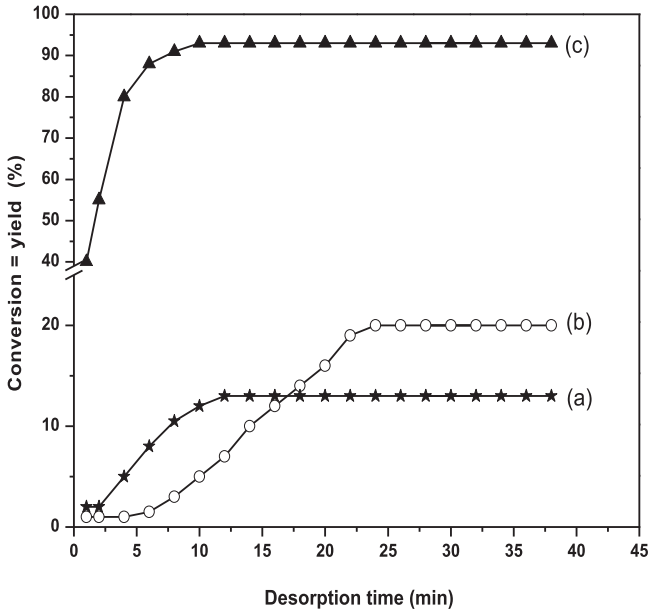

Fig. 4 – Activity variation of IPA with reaction time over presaturated catalysts with acetic acid, (a) pure NiO, (b) pure CuO and (c) CuO mixed with 30 wt.% NiO nanocomposites calcined at 400 °C.

activity over pure CuO. It illustrates that the IPA conversion decreases from 54% to 1% with increasing the volume of acetic acid reaching its steady state after addition of 4 μL. On the other hand curve (c) represents the effect of poisoning the active basic sites CuO mixed with 30 wt.% NiO. It shows that upon addition of acetic acid by 3.5 μL, the conversion activity decreases from 98% to 19%. These results revealed that the acetic acid approximately saturated the available active basic sites responsible for dehydrogenation of IPA over pure oxides whereas 19% is still working in case of the mixed oxide (30 wt.% NiO). In addition, the distribution of the basic sites on the mixed oxide is quite improved.

In an attempt to shed light on the strength of the basic sites over the catalyst presaturated with acetic acid, the activity variation of IPA at the reaction temperature of 200 °C was measured with time and the results are presented in Fig. 4(a–c). Curve (a) shows that desorption of acetic acid from the surface of pure NiO has been almost rapid where the conversion of the IPA and the yield of acetone attained a steady state after 12 min. The value of % conversion and yield of acetone at the steady state was 13% only. This means that about 30% of acetic acid was retained on the catalyst surface as indicated in Fig. 3(a) for the unsaturated NiO. This behavior reflects that the strength of ≈ 71% of the available basic sites on NiO is strong.

Curve 4(b) shows that the desorption of acetic acid from CuO catalyst occurs slowly where the steady state value of conversion was obtained after 25 min. Furthermore, the conversion at the steady state reaches 20% compared to 54% for the unsaturated catalyst. These results reflect that the basicity of CuO catalyst is reduced by 34%. This behavior suggests that the retained acetic acid (34%) on the surface of pure CuO may be due to the presence of ≈ 63% strong basic sites which need higher temperature to overcome the binding energy between the acetic acid and the strong basic sites. According to the results obtained from the desorption of acetic acid from the surfaces of both pure oxides, it is interesting to mention here that the amount of acetic acid retained is approximately equal. This may support that the distribution of the basic sites over both oxide catalysts surfaces almost the same. In addition, the major strength of these sites is strong and uncomfortable for conversion of IPA to acetone.

Curve 4(c) represents the effect of time on the desorption of acetic acid from CuO mixed with 30 wt.% NiO catalyst. It shows that desorption of acetic acid occurs rapidly and hence the conversion of the IPA and the yield of acetone increase rapidly with time. Also, the sample nearly restores its activity ~95% after about 10 minutes. The remained value of ~3% may be attributed to the adsorption of acetic acid on strong basic sites on the catalyst surface.

The comparison between the desorption studies of acetic acid over the catalysts under investigation reveals that CuO mixed with 30 wt.% NiO catalyst restored almost its original activity rapidly compared with CuO and NiO catalysts. This confirms that the creation of weak and intermediate basic sites on the surface of the catalyst containing 30 wt.% NiO enhances the reaction of IPA to acetone and consequently the addition of NiO into CuO promotes its basicity to be comfortable for dehydrogenation of IPA [43–45].

3.3. *Catalytic activity*

The dehydrogenation of IPA over CuO–NiO nanocomposite systems calcined at 400, 500, 600 and 700 °C was carried out and the results are presented in Fig. 5(a). It shows that IPA converts to acetone (major) and propene (minor) over pure CuO and CuO mixed with 1 and 3 wt.% NiO whereas upon

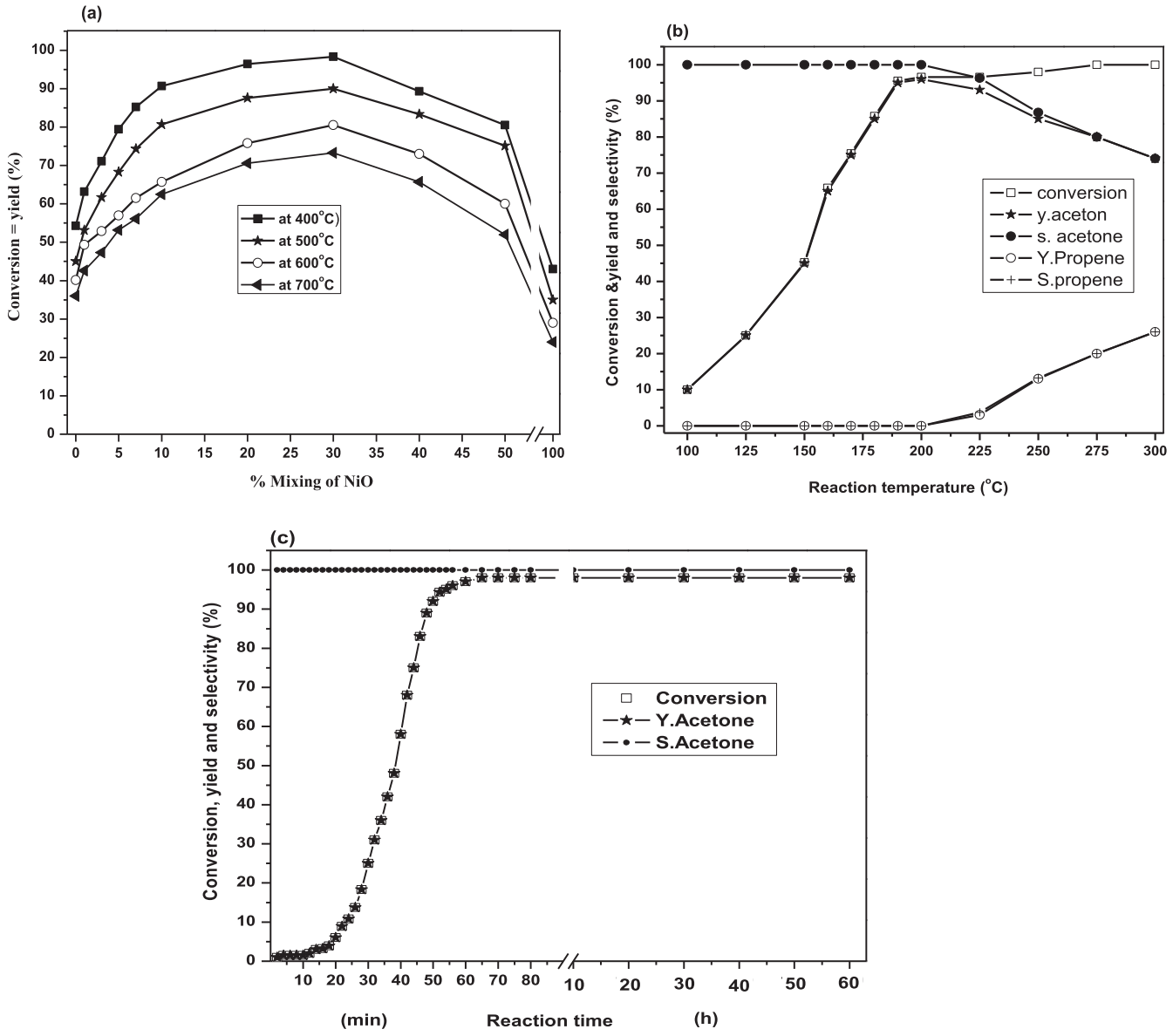

Fig. 5 – (a) Variation of IPA conversion with the % mixing of NiO for CuO–NiO nanocomposite catalysts calcined at 400–700 °C, (b) effect of reaction temperature, and (c) effect of reaction time on the catalytic dehydrogenation of IPA over CuO mixed with 30 wt.% NiO nanocomposites calcined at 400 °C.

increasing the wt.% NiO up to 50%, IPA conversion proceeds to acetone only with selectivity 100%. From these results, one can observe that pure CuO possesses catalytic activity toward IPA conversion to acetone higher than that of pure NiO [46]. Such results may be correlated with the higher values of the surface area and the amount of surface excess oxygen as discussed earlier [28]. On the other hand, it is well known that NiO precedes the dehydrogenation reaction for hydrocarbons and alcohols, thus the formation of acetone as a major product is quite expected. Hence, the observed increase in the selectivity toward acetone formation due to the increase of NiO ratio suggests an increase in the number of active sites responsible for dehydrogenation of IPA. So, the addition of NiO (1–30 wt.%) into CuO as presented in Fig. 5(a) leads to a continuous increase in the conversion of IPA and selectivity toward acetone reaching a maximum yield of (98%) over the catalyst containing 30 wt.% NiO. Above this maximum, further additions of NiO lead to a decrease of both conversion and yield of acetone. The observed remarkable catalytic activity of the mixed oxide catalysts may be not only due to the presence of the one component sites [47,48] Cu^{2+}–Cu^{+}, Ni^{3+}–Ni^{2+}, but also due to the creation of new active ion pairs sites (Cu^{+}–Ni^{3+}). Such active sites which existed via the synergism [17,36–38] are exhibiting weak and intermediate strength as discussed above in the basicity section. The improvement in their strength is playing a major role for the dehydrogenation of IPA. In this context, El-Molla et al. [25] have reported that the presence of medium-strength basic sites on the surface of catalyst catalyzes the rate determining step of the energetically easier H^{α} abstraction from adsorbed 2-propoxide forming carbanion intermediate that finally leads to acetone. In addition, it was reported that Cu^{2+}, Cu^{+} and Cu^{0} are the active and selective sites

responsible for IPA dehydrogenation into acetone over CuO/MgO catalysts [25,49]. They concluded that, at a reaction temperature of 175–275 °C, the different investigated solids behave mainly as a dehydrogenation catalyst yielding acetone beside MIBK (mesityl isobutyl keton) formation via aldol condensation mechanism. At lower temperature, 175 °C, the reaction is completely selective to MIBK, and on increasing the reaction temperature up to and above 200 °C, selectivity to acetone starts to begin reaching to its high value (maximum 92%) at a reaction temperature of 275 °C. Moreover, the catalytic performance of CuO/MgO treated with K_2O catalysts toward IPA conversion, at a reaction temperature of 150–400 °C, was reported [23]. They stated that the system behaved as selective catalyst for dehydrogenation of isopropyl alcohol to acetone (major) with selectivity >80% besides propene as a minor product.

Therefore, from the comparison between our CuO–NiO mixed oxide nanocomposite systems with that previously reported systems [22–27], we can conclude that our system has two advantages: (1) the reaction temperature for complete IPA conversion to acetone, 200 °C, is relatively low compared with the previous reported systems, and (2) the selectivity to acetone as the desired product, reached 100%. These two advantages make our system, which was prepared by a facile route (nanocomposite), a competitive one than those reported previously.

In fact a good contribution of our system for proceeding IPA to acetone may be supported with the results of electrical conductivity as illustrated from the behaviors of both Fig. 5(a) and Fig. 1(a and b) with the wt.% NiO. So, the decrease in ΔE_σ as shown in Table 1 should enhance the electron exchange between IPA and the catalyst surface during the reaction and consequently increases the conversion and selectivity toward acetone formation. Moreover, the decrease in the catalytic activity of the mixed oxides above 30 wt.% may be due to the decrease in their conductivity and the mobility of charge carriers [37]. On increasing the calcination temperature above 400 °C, the results of catalytic activity of the pure and mixed oxides exhibit similar behavior as that observed for the catalysts calcined at 400 °C but with lower values. These results can be discussed in terms of the possible change in the concentration of cation pairs acting as active sites for the catalyzed reaction [50] and a possible decrease in the S_{BET} of the catalysts [28,39,51].

To achieve the best conditions that will give the maximum yield of acetone over the catalyst containing 30 wt.% NiO calcined at 400 °C, the factors affecting the catalytic conversion of IPA into acetone were studied in the following.

3.3.1. *Effect of catalytic reaction temperature*

The effect of reaction temperature on the catalytic conversion of IPA in the range 100–300 °C was studied. The percentages of conversion, yield and selectivity are represented in Fig. 5(b). It shows that the IPA conversion and acetone yield increase monotonically with increasing the reaction temperature reaching the value of 98% at the reaction temperature of 200 °C. Above 200 °C, propene started to appear and it increases with increasing the reaction temperature up to 300 °C. These findings indicate that the active basic sites responsible for the dehydrogenation of IPA are working well at the reaction temperature of 200 °C.

3.3.2. *Effect of catalyst weight*

The effect of the weight of catalyst containing 30 wt.% NiO on the percentages conversion, yield and selectivity of IPA dehydrogenation was studied at 200 °C and the results are shown in Fig. S1, Supplementary material. It shows that the % conversion of IPA increases with increasing the catalyst weigh from (0.1–0.8) reaching its steady state value of 98% with selectivity of 100% toward acetone at a catalyst weight of 0.5 g. These data reflect that as the catalyst weight increases, the number of active basic sites responsible for the dehydrogenation process is normally expected to increase. On further increase in the catalyst weight up to 0.8 g a little amount of propene not exceeding 2% is observed.

3.3.3. *Catalyst stability*

To evaluate the stability of the catalyst containing 30 wt.% NiO, the dehydrogenation of IPA to acetone was investigated and the results are presented in Fig. 5(c). It shows that the maximum conversion of IPA (98%) with selectivity 100% to acetone was obtained after 60 min from the introduction of reactant followed by a steady state till 60 h, which means that the catalyst under test has a good stability toward production of acetone.

4. Conclusions

The main conclusions derived from the results obtained can be summarized as follows:

- Pure and mixed solids of CuO and NiO nanocomposites have been synthesized by direct, facile co-precipitation method (oxalic acid rout).
- The addition of NiO to CuO resulted in increasing the electrical conductivity, whereas the activation energy of conduction decreases.
- Incorporation of NiO with CuO creates more weak and intermediate basic sites which play the main role for the selective dehydrogenation of IPA into acetone.
- The catalyst containing 30 wt.% NiO calcined at 400 °C possesses the highest catalytic activity with 98% conversion and 100% selectivity to acetone at the reaction temperature of 200 °C, and it exhibits good stability with duration time up to 60 h.
- The remarkable activity and selectivity of the catalysts under investigation are correlated well with both electrical conductivity and basicity.

Appendix: Supplementary material

Supplementary data to this article can be found online at doi:10.1016/j.ejbas.2016.08.004.

REFERENCES

[1] Acetone. World petrochemicals report. <http://www.scriconsulting.com/WP/Public/Reports/acetone/>; 2010.

[2] Camera Greiner EO, Funada C. Chemical economic handbook SRI consulting. <http://www.scriconsulting.com/CHE/privat/reports/604.5000/>; June 2010.
[3] Acetone uses and market data. <http://www.icis.com/v2/chemicals/9074858/acetone/uses.html>; 2007.
[4] Zinatloo-Ajabshir S, Salavati-Niasari M. Nanocrystalline Pr_6O_{11}: synthesis, characterization, optical and photocatalytic properties. New J Chem 2015;39:3948–55.
[5] Zinatloo-Ajabshir S, Salavati-Niasari M. Preparation of nanocrystalline cubic ZrO_2 with different shapes via a simple precipitation approach. J Mater Sci 2016;27:3918–28.
[6] Zinatloo-Ajabshir S, Salavati-Niasari M, Hamadanian M. Praseodymium oxide nanostructures: novel solvent-less preparation, characterization and investigation of their optical and photocatalytic properties. RSC Adv 2015;5:33792–800.
[7] Moshtaghi S, Zinatloo-Ajabshir S, Salavati-Niasari M. Preparation and characterization of $BaSnO_3$ nanostructures via a new simple surfactant-free route. J Mater Sci 2016;27:425–35.
[8] Zinatloo-Ajabshir S, Salavati-Niasari M. Zirconia nanostructures: novel facile surfactant-free preparation and characterization. Int J Appl Ceram Technol 2016;13:108–15.
[9] Zinatloo-Ajabshir S, Salavati-Niasari M. Novel poly(ethyleneglycol)-assisted synthesis of praseodymium oxide nanostructures via a facile precipitation route. Ceram Int 2015;4:567–75.
[10] Zinatloo-Ajabshir S, Salavati-Niasari M. Preparation and characterization of nanocrystalline praseodymium oxide via a simple precipitation approach. J Mater Sci 2015;26:5812–21.
[11] Khaleel A, Shehadil I, Al-Shamisi M. Nanostructured chromium–iron mixed oxides: physicochemical properties and catalytic activity. Colloids Surf A Physicochem Eng Asp 2010;355:75–82.
[12] Zhang YX, Kuanga M, Wang JJ. Mesoporous CuO–NiO micropolyhedrons: facile synthesis, morphological evolution and pseudocapcitive performance. CrystEngComm 2014;16:492–8.
[13] Cao J-L, Wang Y, Yu X-L, Wang S-R, Wu S-H, Yuan Z-Y. Mesoporous CuO-Fe_2O_3 composite catalysts for low temperature carbon monoxide oxidation. Appl Catal B 2008;79:26–34.
[14] El-Shobaky GA, Radwan NRE, El-Shall MS, Turky AM, Hassan HMA. Physicochemical, surface and catalytic properties of nanocrystalline CuO–NiO system as being influenced by doping with La_2O_3. Colloids Surf A Physicochem Eng Asp 2009;345:147–54.
[15] El-Shobaky GA, Radwan NRE, El-Shall MS, Turky AM, Hassan HMA. Synthesis and characterization of pure and ZrO_2-doped nanocrystalline CuO–NiO system. Appl Surf Sci 2008;254:1651–60.
[16] Chang FC, Liao PH, Tsai CK, Hsiao MC, Wang HP. Chemical-looping combustion of syngas with nano CuO-NiO on chabazite. Appl Energy 2014;113:1731–6.
[17] El-Shobaky GA, Radwan NRE, El-Shall MS, Turky AM, Hassan HMA. The role of method of preparation of CuO–NiO system on its physicochemical surface and catalytic properties. Colloids Surf A Physicochem Eng Asp 2007;311:161–9.
[18] El-Shobaky GA, Hewaidy IF, El-Nabarawy T. Effects of stoichiometric composition and surface characteristics on the catalytic activity of CoO catalyst. Surf Technol 1980;10:225–33.
[19] Luo J, Xu H, Liu Y, Chu W, Jiang C, Zhao X. Facile approach for the preparation of biomorphic CuO–ZrO_2 catalyst for catalytic combustion of methane. Appl Catal A Gen 2012;423–424:121–9.
[20] Ahmadi TS, Wang LZ, Green CT, Henglein A, El-Sayed AM. Shape-controlled synthesis of colloidal platinum nanoparticles. Science 1996;272:1924–5.
[21] Glaspell G, Fuoco L, El-Shall MS. Microwave synthesis of supported Au and Pd nanoparticle catalysts for CO oxidation. J Phys Chem B 2005;109:17350–5.
[22] Turton R, Baili R, Whiting W, Shaeiwitz J. Analysis, synthesis and design of chemical processes. Prentice-Hall; 1988.
[23] El-Molla SA, El-Shobaky GA, Amin NH, Hammed MN, Sultan SN. Catalytic properties of pure and K-doped CuO/MgO system towards 2-propanol conversion. J Mex Chem Soc 2013;57:36–42.
[24] Ashour SS. Structural, textural and catalytic properties of pure and Li-doped NiO/Al_2O_3 and CuO/Al_2O_3 catalysts. J Saudi Chem Soc 2014;18:69–76.
[25] El-Molla SA, Abdel-all SM, Ibrahim MM. Influence of precursor of MgO and preparation conditions on the catalytic dehydrogenation of isopropanol over CuO/MgO catalysts. J Alloys Compd 2009;484:280–5.
[26] Deraz NM, Al-Arifi A. Preparation and physicochemical properties of individual and binary Ni and Ce oxides system. Polyhedron 2010;29:3277–82.
[27] Shaheen WM, Zahran AA, El-Shobaky GA. Surface and catalytic properties of NiO/MgO system doped with Fe_2O_3. Colloids Surf A Physicochem Eng Asp 2003;231:51–65.
[28] Said AA, Abd El-Wahab MM, Soliman SA, Goda MN. Synthesis and characterization of nano CuO-NiO mixed oxides. Nanosci Nanoeng 2014;2:17–22.
[29] Wang X, Song J, Gao L, Jin J, Zheng H, Zhang Z. Optical and electrochemical properties of nanosized NiO via thermal decomposition of nickel oxalate nanofibres. Nanotechnology 2005;16:37–9.
[30] Li G-J, Huang X-X, Shi Y, Guo J-K. Preparation and characteristics of nanocrystalline NiO by organic solvent method. Mater Lett 2001;51:325–30.
[31] Said AA, Hassan EA, Abd El-Salam KM. Electrical conductivity and thermogravimetric studies of the thermal decomposition of doped cobalt carbonate. Surf Technol 1983;20:123–30.
[32] Boreskov GK. Catalytic activity of transition metal compounds in oxidation reactions. In: Hightower JW, editor. 5th International congress on catalysis, vol. 2. Amsterdam: North-Holland; 1973. p. 981–90.
[33] Kostad P. Non-stoichiometry, diffusion and electrical conductivity in Binary Metal Oxides. New York: Wiley-Interscience; 1972.
[34] Salem AM, Mokhtar M, El-Shobaky GA. Electrical properties of pure and Li_2O-doped NiO/MgO system. Solid State Ion 2004;170:33–42.
[35] Turky G, Selim MS, El-Shobaky GA. Electrical properties of pure and Li_2O-doped CuO/Fe_2O_3 system precalcined at different temperatures. Solid State Ion 2001;140:395–403.
[36] Deraz NM. Physicochemical, surface, and catalytic properties of pure and Ceria-Doped manganese/alumina catalysts. Chin J Catal 2008;29:687–95.
[37] Deraz NM. Effect of NiO content on structural, surface and catalytic characteristics of nano-crystalline NiO/CeO_2 system. Ceram Int 2012;38:747–53.
[38] Deraz NM. Effects of heat treatment on physicochemical properties of cerium based nickel system. J Anal Appl Pyrolysis 2012;95:56–60.
[39] Said AA, Abd El-Wahab MM, Soliman SA, Goda MN. Synthesis and characterization of mesoporous Fe-Co mixed oxide nanocatalysts for low temperature CO oxidation. Process Saf Environ Prot 2016;102:370–84.
[40] Abd El-Salaam KM, Said AA, El-Awad AM, Hassan EA, Abd El-Wahab MM. Structure and electronic effects of cobalt ferrites, $Co_xFe_{3-x}O_4$, on catalytic decomposition of isopropyl alcohol. Collect Czech Chem Commun 1994;59:1939–50.
[41] Morrison SR. Chemical physics of surfaces. New York: Plenum; 1978. p. 70.

[42] Hauffe K. The application of the theory of semiconductors to problems of heterogeneous catalysis. Adv Catal 1955;7:213–57.
[43] Said AA, Abd El-Wahab MM. Surface properties and catalytic behavior of MoO_3/SiO_2 in esterification of acetic acid with ethanol. J Chem Technol Biotechnol 2006;81:329–35.
[44] Said AA, Abd El-Wahab MM, Alian MA. Catalytic performance of Brønsted acid sites during esterification of acetic acid with ethyl alcohol over phosphotungstic acid supported on silica. J Chem Technol Biotechnol 2007;82:513–23.
[45] Said AA, Abd El-Wahab MM, Abd El Aal M. The catalytic performance of sulfated zirconia in the dehydration of methanol to dimethyl ether. J Mol Catal A Chem 2014;394:40–7.
[46] Kulkarni D, Wachs IE. Isopropanol oxidation by pure metal oxide catalysts: number of active surface sites and turnover frequencies. Appl Catal A Gen 2002;237:121–37.
[47] El-Shobaky HG, Shaheen WM. Effect of γ-irradiation and doping with MoO_3 and V_2O_5 on surface and catalytic properties of manganese oxides. Radiat Phys Chem Oxf Engl 1993 2003;66:55–65.
[48] Shaheen WM. Thermal solid–solid interactions and physicochemical properties of NiO/Fe_2O_3 system doped with K_2O. Thermochim Acta 2008;470:18–26.
[49] El-Molla SA. Dehydrogenation and condensation in catalytic conversion of isopropanol over CuO/MgO system doped with Li_2O and ZrO_2. Appl Catal A Gen 2006;298:103–12.
[50] Radwan NRE, Mokhtar M, El-Shobaky GA. Surface and catalytic properties of CuO and Co_3O_4 solids as influenced by treatment with Co^{2+} and Cu^{2+} species. Appl Catal A Gen 2003;241:77–90.
[51] El-Molla SA, Hammed MN, El-Shobaky GA. Catalytic conversion of isopropanol over NiO/MgO system doped with Li_2O. Mater Lett 2004;58:1003–11.